Non-uniform magnetic field-induced performance alteration of a topology-optimized PBMR

Debdeep Bhattacherjee[1], Arnab Atta[1], Suman. Chakraborty[2]
1. Department of Chemical Engineering, Indian Institute of Technology Kharagpur, Kharagpur, WB, India.
2. Department of Mechanical Engineering, Indian Institute of Technology Kharagpur, Kharagpur, WB, India.

Abstract
Packed bed microreactors (PBMR) and ferrofluids are independently enormously used in a broad range of applications in the healthcare sector. In a PBMR, one of the primary factors for controlling the reaction rate is the bed porosity which immediately affects the catalyst distribution and the reactant flow [1]. When exploiting ferrofluid as the reactant, an alternative approach is offered to regulate the flow in microreactors by employing external magnetic fields alongside the impact of pressure-driven flow. Intensifying mass transport inside a PBMR is rendered attainable by the application of ferrofluid reactants. As an example, for the extraction of succinic acid from n-butanol to water inside a laminar flow microreactor (e.g., PBMR), the addition of ferrofluids regulated by an external fixed magnetic field was shown to significantly increase the overall mass transfer coefficient considerably up to 70% [2]. On the contrary, periodic variations in ferrofluid velocity triggered by the applied magnetic field have a negative impact on the liquid-solid mass transfer [3]. To enhance the mass transfer rate within a PBMR, further magnetic field manipulation and catalyst distribution optimization are recommended. The topology optimization method, one of the most prevalent approaches, spatially optimizes the ordering of the material within a specific domain by minimizing a predetermined cost function and attaining specified constraints. In the present work, we provide a topology optimization method for improving the reaction conversion by achieving an ideal catalyst bed porosity for ferrofluid reactants and including the external non-uniform magnetic field that additionally modifies the optimized reaction conversion. To provide a fundamental understanding, we considered a first-order reaction in a tubular microreactor and expanded the influence of the magnetic field intensity on the average bed porosity and reaction conversion. To accomplish the objectives, we employed the finite element method-based solver COMSOL Multiphysics. We utilized the 'Fluid Flow' module of the COMSOL Multiphysics software to solve the flow field, the 'Chemical Species Transport' module for the reaction kinetics, and the 'AC/DC' module for the magnetic field analysis. The outcomes from the simulation demonstrated that the addition of a non-uniform magnetic field may regulate the optimization process, and as a consequence, depending on the field orientation, we may attain either a higher or lower conversion in comparison to the optimum conversion in the absence of a magnetic field.

Keywords: PBMR, Magnetic field, Topology optimization.

Introduction
Chemical reaction engineering plays a crucial role in both the medical and industrial sectors [4]. The chemical reactions occur inside open channels in millimeter-sized PBMRs, characterized by laminar flow [5]. The use of PBMRs offers various advantages compared to the utilization of conventional reactors, with one notable advantage being their improved surface-to-volume ratio [1]. An alternative approach to regulating the flow inside microreactors is shown via the use of ferrofluid as the reactant. This approach integrates the influences of external magnetic fields with pressure-driven flow. The use of ferrofluid reactants facilitates the enhancement of mass transfer inside PBMRs depending on their directions. For example, previous studies have shown that the utilization of ferrofluids, which are manipulated by an externally applied magnetic field, significantly enhances the overall mass transfer coefficient by up to 70% [2]. This improvement is observed specifically during the extraction process of succinic acid from n-butanol into water, which takes place within a laminar flow microreactor, such as the PBMR. Conversely, the fluctuating velocity of ferrofluid induced by the magnetic field application negatively impacts the process of liquid-to-solid mass transfer [3].

The primary emphasis in previous studies has been on the design of reactor structures and the development of catalysts to enhance the reaction process [6]–[8]. The adoption of simplified techniques often poses challenges in achieving optimal microreactor efficiency, since it is heavily impacted by the spatial arrangement of catalysts inside the reactor. Increasing the flow rate of reactants and the quantity of catalyst used may effectively augment the rate of the reaction. To maintain the increased reactant input rate, it is necessary to maximize the catalyst bed porosity (ε), which is defined as the volume fraction occupied by the reactant. Nevertheless, it is essential to minimize the value of ε to enable the reactor to effectively maintain a significant quantity of catalysts. To achieve the best conversion rate, it is essential to establish an optimal catalyst distribution pattern that effectively addresses the inherent contradiction between these two factors. The consideration of bed porosity is crucial in reactor design due to its direct influence on catalyst placement and reactant movement. Desmet et al. [9] provided a more comprehensive analysis of the optimal distribution of solid catalysts inside the reactor to enhance the pace of reaction in this particular context. The researchers considered a porous monolithic bed

reactor characterized by laminar flow and an isothermal first-order reaction. Okkels and Bruus [10] conducted computer simulations on the catalyst dispersion in a two-dimensional reactor to enhance the yield of a first-order reaction, assuming the reactant to possess Newtonian fluid properties.

The topology optimization technique (TOM) is well recognized as a common approach for discovering the optimal arrangement of catalysts [11]. The use of this technology has been seen throughout a diverse range of scientific and technological domains, including channel design, acoustics, and optical research, as well as several production procedures within the aerospace and automotive industries [12]–[14]. The Targeted Optimization Method (TOM) is an analytical approach that aims to enhance the geographic distribution of a given element within a defined region of interest. This is achieved by minimizing a pre-established cost function while simultaneously satisfying certain constraints. The method of moving asymptotes (MMA) is a commonly used iterative approach for addressing TOM issues [15].

The reactants were regarded as Newtonian and non-magnetic fluids in the majority of the published research. A broad variety of magnetic reactants are, however, also often utilized in reactive flows, where the fluid flow is directly influenced by the external magnetic field. A numerical investigation was conducted in this work to ascertain the optimal distribution of catalysts for magnetic reactants. The study included the evaluation of a traditional axisymmetric tubular reactor configuration. This reactor operates under the conditions of a single-phase first-order reaction, facilitated by the presence of porous catalysts with adjustable porosity (ε). The ability to independently control the porosity inside the reactor was a key factor under consideration. The objective of this optimization is to improve reactor efficiency by determining the most effective distribution of catalysts inside the reactor, considering a pressure-gradient-driven flow.

Problem formulation and methodology

Figure 1 illustrates the layout of the microreactor under consideration, which facilitates a first-order catalytic reaction inside a porous bed. In a recent publication, we used a comparable reactor configuration, whereby we strategically tuned the dispersion of catalysts to get maximum conversion rates for various non-Newtonian and non-magnetic reactants [1]. In this particular case, solid catalysts are used to facilitate the catalytic transformation of the reactant (R) into the desired product (P) as

$$\mathrm{R} \xrightarrow[\textit{inside the microreactor}]{\textit{solid porous catalyst bed}} \mathrm{P}$$

The offered system allows for the representation of the steady-state advection-diffusion reaction kinetics equation using Eq. (1).

$$[\mathbf{u}(\varepsilon)\cdot\boldsymbol{\nabla}]\mathrm{C}_r = \mathrm{D}\boldsymbol{\nabla}^2\mathrm{C}_r - \mathrm{k}_c(\varepsilon)\mathrm{C}_r \qquad (1)$$

Here, C_r is the concentration of the reactant, $\mathbf{u}(\varepsilon)$ is the reactant velocity through the porous catalyst bed, D is the diffusion coefficient of the reactant, $\mathrm{k}_c(\varepsilon)$ is the rate constant of the first-order reaction, where $\mathrm{k}_c(\varepsilon)\ \alpha\ (1-\varepsilon)$ [16]. The boundary conditions are

$$\left.\begin{aligned} &\text{inlet: } \mathrm{C}_r|_{r,z=0} = \mathrm{C}_{r,0} \\ &\text{wall: } \left.\frac{\partial \mathrm{C}_r}{\partial r}\right|_{r=3\mathrm{L},z} = 0 \\ &\text{outlet: } \left.\frac{\partial \mathrm{C}_r}{\partial r}\right|_{r=0,z=10\mathrm{L}} = 0 \end{aligned}\right\} \qquad (2)$$

Additionally, the reactant flow is governed by the continuity and momentum equations as [1]

$$\left.\begin{aligned} &\boldsymbol{\nabla}\cdot\mathbf{u}(\varepsilon) = 0 \\ &\rho[\mathbf{u}(\varepsilon)\cdot\boldsymbol{\nabla}]\mathbf{u}(\varepsilon) = -\boldsymbol{\nabla}\mathrm{p} + \eta\boldsymbol{\nabla}^2\mathbf{u}(\varepsilon) + \mathbf{F}_{mag} - \alpha(\varepsilon)\mathbf{u}(\varepsilon) \end{aligned}\right\} \qquad (3)$$

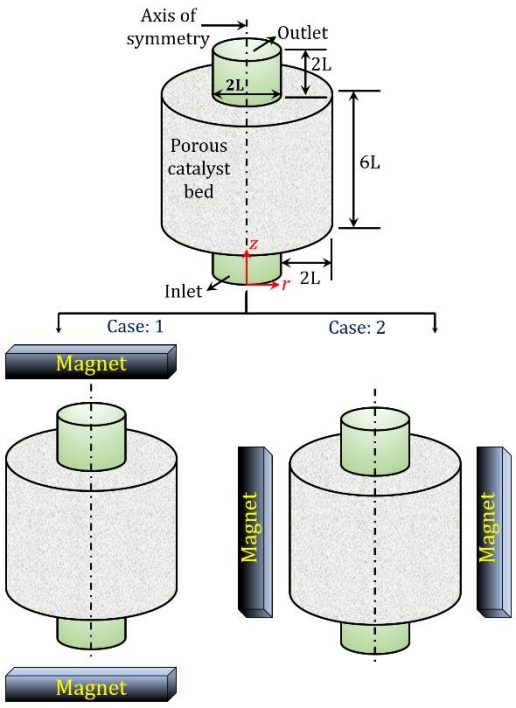

Figure 1. Diagram of the axisymmetric reactor under consideration, packed with solid porous catalysts (here L *= 1 mm).*

Here, ρ is the reactant density, η is the fluid viscosity, $\mathbf{F}_{mag} = \boldsymbol{\nabla}\cdot\left(\mu\mathbf{H}\mathbf{H}^{\mathrm{T}} - \frac{\mu}{2}|\mathbf{H}|^{\mathbf{2}}\mathbf{I}\right)$ is the force due to the external magnetic field that follows the magneto-static Maxwell equations [see Eq. (4)], $\alpha(\varepsilon) = \alpha_{max}\{\mathrm{q}(1-\varepsilon)/(\mathrm{q}+\varepsilon)\}$ is the local inverse permeability, q is the global convergence positive parameter, and α_{max} depends on Darcy number (Da) as $\alpha_{max} = \eta/(\mathrm{Da}\,\mathrm{L}^2)$.

$$\left.\begin{aligned}\nabla \cdot \mathbf{B} &= 0\\ \nabla \times \mathbf{H} &= 0\\ \mathbf{M} &= \chi \mathbf{H}\\ \mathbf{B} &= \mu \mathbf{H}\end{aligned}\right\} \quad (4)$$

where **B** is the magnetic induction, **H** is the magnetic field, **M** is the magnetization, χ is the magnetic susceptibility of the reactant, $\mu = \mu_0(1+\chi)$ is the magnetic permeability, and μ_0 is the permeability of the vacuum.

The boundary conditions of Eq. (3) are

$$\left.\begin{aligned}&\text{inlet: } \mathrm{p} = \mathrm{p}_{in} \text{ at } z = 0\\ &\text{outlet: } \mathrm{p} = 0 \text{ at } z = 10\mathrm{L}\end{aligned}\right\} \quad (5)$$

In the optimization technique, we have introduced an objective function $\psi(\varepsilon) = -(\mathrm{k}_c(\varepsilon)\mathrm{C}_r)|_{mean}$, which has to be minimized. Furthermore, Okkels and Bruus stated the objective function as follows when the reactor was assumed to be non-diffusive (D = 0) [1]

$$\psi(\varepsilon) = -\frac{\mathbf{u}(\varepsilon)\mathrm{C}_0}{\mathrm{L}}\mathrm{X}_r \quad (6)$$

where $\mathrm{X}_r = (\mathrm{C}_0 - \mathrm{C}_f)/\mathrm{C}_0$ and $\mathbf{u}(\varepsilon) = (\mathrm{Da}\ \Delta\mathrm{p}\ \mathrm{L})/((1-\varepsilon)\eta)$.

The numerical simulations were conducted using COMSOL Multiphysics, a solver based on the finite element technique. The moving asymptotes technique (MMA) was used in our study to conduct topology optimization. The procedural flow for the topology optimization methodology used in this study is shown in Figure 2. In addition, the COMSOL Multiphysics software was used to address the flow field, reaction kinetics, magnetic field, and optimization techniques using its 'Fluid Flow', 'Chemical Species Transport', 'AC/DC', and 'Mathematics' modules, respectively. The details of the COMSOL modules used for the simulation are supplied in tabular form in the Appendix.

Results and discussion

Grid independence study

A grid independence test was run prior to conducting model confirmation and parametric tests to determine the optimal mesh size that produces accurate results within an adequate simulation period. The computational domain was integrated utilizing freely available triangle components. Table 1 presents the important factors associated with the grid independence test.

The velocity curves at the entry of a nonreactive system were examined in the absence of a porous bed (ε = 1) and magnetic field [1]. The findings are shown in Figure 3. For the rest of our investigation,

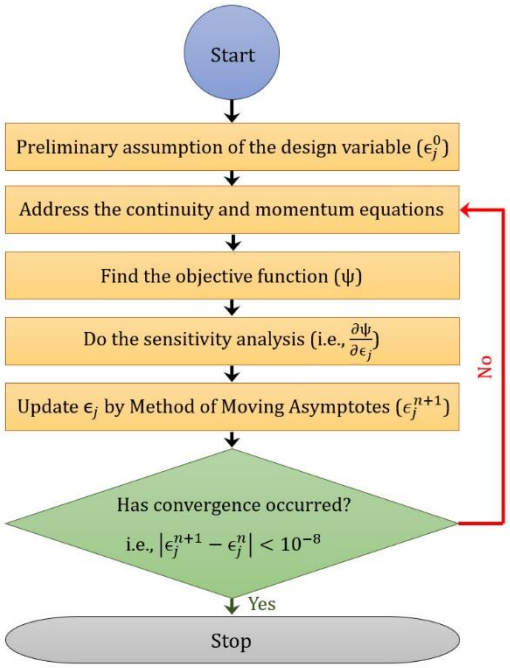

Figure 2. Flow chart for the topology optimization process [1].

Grid M4 has been selected due to the ignorable variation (less than 1%) in velocity profiles between Grids M4 and M5.

Table 1: *Mesh information for the grid independence test.*

Grid	Maximum grid size (in mm)	Difference with M5 (in percentage)
M1	0.260	4.11
M2	0.135	1.83
M3	0.085	1.15
M4	0.039	0.26
M5	0.020	–

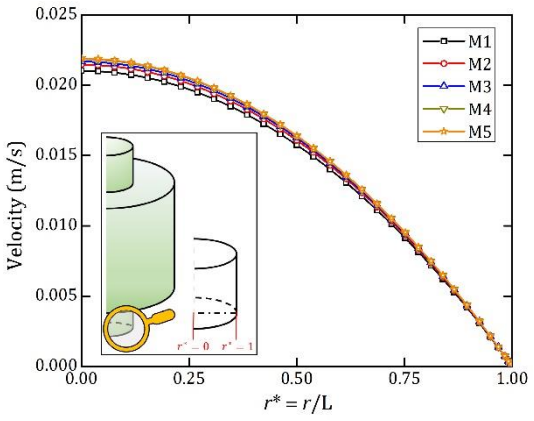

Figure 3. Dependency of the inlet velocity profiles along the radial direction on the meshing. Other parameters are ε = 1, Δp = 0.5 Pa, η = 0.001 Pa s, *and in the absence of a magnetic field.*

Model verification

To validate our model, we used established numerical techniques from existing literature that have been previously utilized for non-diffusing and

Newtonian systems. Here, we explored our two-dimensional axisymmetric geometry with similar dimensional geometry available in the literature [1], [10]. The model parameters used in this study are shown in Table 2

Table 2: *Parameters for the model validation.*

Variable \ $\frac{\sqrt{\tau_A\tau_R}}{\tau_D}$	**0.379**	**0.190**	**0.141**	**0.089**
Da	10^{-4}	10^{-4}	10^{-5}	10^{-4}
D (m^2/s)	3×10^{-8}	3×10^{-8}	10^{-8}	10^{-8}
Δp (Pa)	0.25	0.25	0.5	0.25
k_c (1/s)	0.25	1	1	0.5

Okkels and Bruus [10] proposed a framework consisting of three unique characteristic time scales, namely τ_A, τ_R, and τ_D, representing the notions of advection, reaction, and diffusion, respectively. Then, under the condition of weak diffusion, they presented a dimensionless scaling parameter as $\frac{\sqrt{\tau_A\tau_R}}{\tau_D} = \frac{\mathrm{D}}{\sqrt{k_c(\varepsilon)\mathbf{u}(\varepsilon)L^3}}$. This comparison (refer to Fig. 4) shows that our model exhibits strong agreement with their outcomes, as shown by a maximum deviation of 9.43% in our model predictions. Similar to their finding, we too discovered that the reaction conversion grew with $\frac{\sqrt{\tau_A\tau_R}}{\tau_D}$ up to a certain number, and then it constantly fell. This phenomenon may be attributed to the adjustment of the rate constant value, which was optimized for the given topology. All further parametric tests were conducted with $\frac{\sqrt{\tau_A\tau_R}}{\tau_D} = 0.141$ since this value yielded the greatest conversion rate in our system. Additionally, due to its ability to accurately represent and interpret a three-dimensional visual perception, we have deemed it helpful to further examine the two-dimensional axisymmetric model for potential future research.

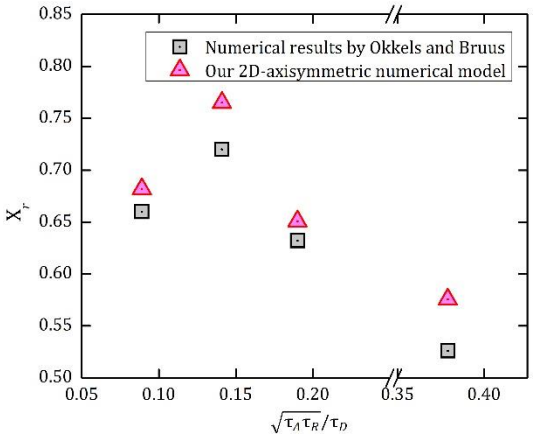

Figure 4. Model validation with the numerical results of Okkels and Bruus for Newtonian fluids (η = 0.001 Pa s *and* ρ = 1000 kg/m^3).

Effect of non-uniform magnetic fields

Here, we will examine the distribution of catalysts and concentration contours following the introduction of non-uniform magnetic fields. Initially, we acquired optimal axisymmetric microreactors. Subsequently, we analyzed the effects of non-uniform magnetic field strengths on the fluid dynamics inside the microreactor. This parameter plays a crucial role in determining the distribution of catalysts and the conversion of reactions. In this research, we examined two separate scenarios: firstly, the application of a magnetic field in the vertical direction (along the $z-$axis), and secondly, the introduction of a magnetic field in the horizontal direction (along the $r-$axis) [refer to Fig. (1)]. Table 3 provides a summary of all the variables associated with the simulations.

Table 3: *variables employed in simulations.*

Variable	**Value**
Da	10^{-5}
D (m^2/s)	10^{-8}
Δp (Pa)	0.5
k_c (1/s)	1
C_0 (mol/m^3)	1
ρ (kg/m^3)	1000
η (Pa s)	0.001
χ	0.5

Figures 5(a) and (b) illustrate the relationship between reaction conversion and catalyst distribution under varying field strengths for both scenarios. When comparing case-1 with case-2, the data shown in the figure supports the conclusion that the vertical location of the magnetic field consistently leads to higher reaction conversion and average bed porosity compared to the horizontal magnetic field.

In contrast, the conversion of the reaction and the average porosity of the bed exhibit an increase with the intensity of the magnetic field in case-1, whereas they show a reduction with the field strength in case-2. The purpose of this study is to minimize the objective function [ψ(ε)], which may be interpreted as maximizing the velocity field [$\mathbf{u}(\varepsilon)$] to improve the performance of the reactor. Hence, in the first scenario, the manipulation of H within the range of 0 to 500 A/m resulted in an escalation of the velocity inside the reactor, requiring augmentation of the bed porosity to achieve optimum performance. This phenomenon increases the flow field, leading to an enhancement in the conversion of the reaction. Conversely, in the case-2, there is a dramatic shift in the other direction.

Figure 7 depicts the configuration of the typical distribution of reactant concentrations in topology-optimized reactors with a magnetic field strength of

H = 500 A/m, in both scenarios with and without the presence of a magnetic field.

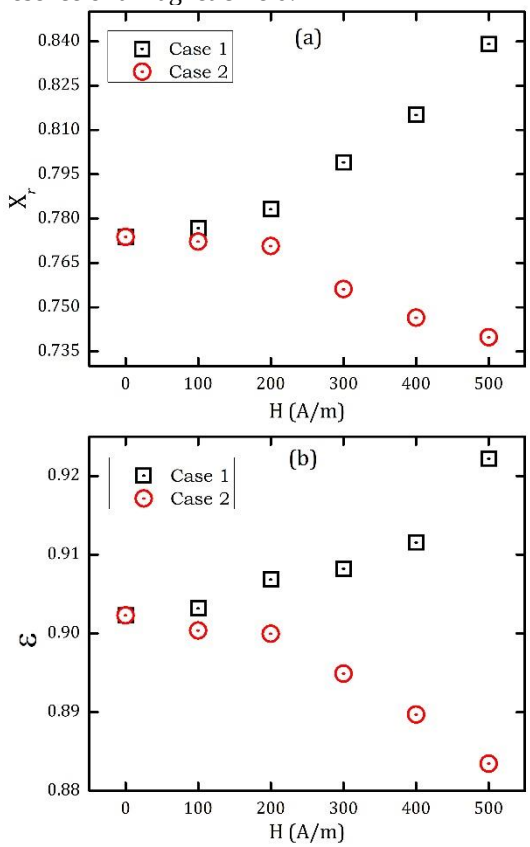

Figure 5. Variation of (a) reaction conversion (X_r) *and (b) volume average catalyst-bed porosity* (ε) *with the magnetic field strength (*H *in* A/m*).*

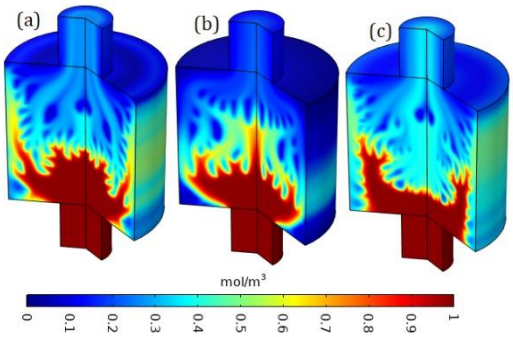

Figure 7. Representative illustration of the model predictions showing the distribution of reactant concentration (mol/m3) in the topology-optimized reactor for (a) no magnetic field, (b) case-1 at H = *500* A/m, *and (c) case-2 at* H = *500* A/m.

Conclusions

In this study, we provide a methodology for topology optimization aimed at enhancing the conversion of reactions. Our approach involves establishing an optimal porosity for the catalyst bed used in ferrofluid reactions, while also considering the influence of an external non-uniform magnetic field on the improved reaction conversion. The results obtained from the simulation indicate that the inclusion of a non-uniform magnetic field can influence the optimization process. Depending on the orientation of the field, it is possible to achieve either a higher or lower conversion rate compared to the optimal conversion rate in the absence of a magnetic field.

Acknowledgments

S.C. acknowledges the Department of Science and Technology, Government of India, for Sir J. C. Bose National Fellowship.

Nomenclature

ε	Catalyst bed porosity [-]
u	Reactant velocity [m/s]
C_r	Reactant concentration [mol/m^3]
D	Diffusion coefficient [m^2/s]
k_c	Rate constant [1/s]
ρ	Reactant fluid density [kg/m^3]
Δp	Pressure difference [Pa]
η	Reactant fluid viscosity [Pa s]
L	Characteristic length [mm]
Da	Darcy number [-]
X_r	Reaction conversion [-]
C_0	Initial concentration of the reactant [mol/m^3]
C_f	Final concentration of the reactant [mol/m^3]
H	Applied magnetic field strength [A/m]
χ	Magnetic susceptibility of the reactant [-]

Abbreviation

PBMR	Packed bed microreactors
TOM	Topology optimization method
MMA	Method of moving asymptotes

Appendix

Module	**Sub module**	**Input variable**
Fluid Flow	Laminar Flow (*spf*)	Fluid Properties
		Inlet
		Outlet
		Wall
		Volume Force
Chemical Species Transport	Transport of Diluted Species (*tds*)	Transport Properties
		Inlet
		Outflow
		No Flux
		Reactions
AC/DC	Magnetic Fields, No Currents (*mfnc*)	Magnetic Flux Conservation
		Magnetic Insulation
		Magnetic Flux Density
		Zero Magnetic Scalar Potential
Mathematics	Optimization (*opt*)	Control Variable Field
		Integral Objective

References

[1] D. Bhattacharjee and A. Atta, "Topology optimization of a packed bed microreactor involving pressure driven non-Newtonian fluids," *Reaction Chemistry & Engineering*, vol. 7, no. 3, pp. 609–618, 2022.

[2] N. Azimi, M. Rahimi, and N. Abdollahi, "Using magnetically excited nanoparticles for liquid–liquid two-phase mass transfer enhancement in a Y-type micromixer," *Chemical Engineering and Processing: Process Intensification*, vol. 97, pp. 12–22, 2015.

[3] P. Lisk *et al.*, "Magnetic actuation of catalytic microparticles for the enhancement of mass transfer rate in a flow reactor," *Chemical Engineering Journal*, vol. 306, pp. 352–361, 2016.

[4] K. Wang, L. Li, P. Xie, and G. Luo, "Liquid–liquid microflow reaction engineering," *Reaction Chemistry & Engineering*, vol. 2, no. 5, pp. 611–627, 2017.

[5] S. Rebughini, M. Bracconi, A. G. Dixon, and M. Maestri, "A hierarchical approach to chemical reactor engineering: an application to micro packed bed reactors," *Reaction Chemistry & Engineering*, vol. 3, no. 1, pp. 25–33, 2018.

[6] C. Cao, G. Xia, J. Holladay, E. Jones, and Y. Wang, "Kinetic studies of methanol steam reforming over Pd/ZnO catalyst using a microchannel reactor," *Applied Catalysis A: General*, vol. 262, no. 1, pp. 19–29, 2004.

[7] C. Cao, Y. Wang, J. D. Holladay, E. O. Jones, and D. R. Palo, "Design of micro-scale fuel processors assisted by numerical modeling," *AIChE Journal*, vol. 51, no. 3, pp. 982–988, 2005.

[8] S. K. Ajmera, M. W. Losey, K. F. Jensen, and M. A. Schmidt, "Microfabricated packed-bed reactor for phosgene synthesis," *AIChE Journal*, vol. 47, no. 7, pp. 1639–1647, 2001.

[9] G. Desmet, J. De Greef, H. Verelst, and G. V. Baron, "Performance limits of isothermal packed bed and perforated monolithic bed reactors operated under laminar flow conditions. I. General optimization analysis," *Chemical Engineering Science*, vol. 58, no. 14, pp. 3187–3202, 2003.

[10] F. Okkels and H. Bruus, "Scaling behavior of optimally structured catalytic microfluidic reactors," *Physical Review E*, vol. 75, no. 1, p. 016301, 2007.

[11] L. H. Olesen, F. Okkels, and H. Bruus, "A high-level programming-language implementation of topology optimization applied to steady-state Navier–Stokes flow," *International Journal for Numerical Methods in Engineering*, vol. 65, no. 7, pp. 975–1001, 2006.

[12] C. B. W. Pedersen, T. Buhl, and O. Sigmund, "Topology synthesis of large-displacement compliant mechanisms," *International Journal for Numerical Methods in Engineering*, vol. 50, no. 12, pp. 2683–2705, 2001.

[13] J. S. Jensen and O. Sigmund, "Systematic design of photonic crystal structures using topology optimization: Low-loss waveguide bends," *Applied Physics Letters*, vol. 84, no. 12, pp. 2022–2024, 2004.

[14] H. R. E. M. Hörnlein, M. Kočvara, and R. Werner, "Material optimization: bridging the gap between conceptual and preliminary design," *Aerospace Science and Technology*, vol. 5, no. 8, pp. 541–554, 2001.

[15] K. Svanberg, "The method of moving asymptotes—a new method for structural optimization," *International Journal for Numerical Methods in Engineering*, vol. 24, no. 2, pp. 359–373, 1987.

[16] T. E. Bruns, O. Sigmund, and D. A. Tortorelli, "Numerical methods for the topology optimization of structures that exhibit snap-through," *International Journal for Numerical Methods in Engineering*, vol. 55, no. 10, pp. 1215–1237, 2002.